PENSOFT

SENCKENBERG
world of biodiversity

Leibniz Association

To see the unseen: notes on the larval morphology and systematic position of *Achanthiptera* Rondani (Diptera: Muscidae)

Kinga Walczak[1,2], Thomas Pape[3], James F. Wallman[4,5], Krzysztof Szpila[1], Andrzej Grzywacz[1,2]

1 *Department of Ecology and Biogeography, Faculty of Biological and Veterinary Sciences, Nicolaus Copernicus University in Toruń, Poland*

2 *Centre for Modern Interdisciplinary Technologies, Nicolaus Copernicus University in Toruń, Poland*

3 *Natural History Museum of Denmark, University of Copenhagen, Copenhagen, Denmark*

4 *Faculty of Science, University of Technology Sydney, Ultimo, NSW, Australia*

5 *School of Earth, Atmospheric and Life Sciences, University of Wollongong, Wollongong, NSW, Australia*

https://zoobank.org/AB3BBC89-3032-4827-B39A-0EB3086E4086

Corresponding authors: Kinga Walczak (walczak.kinga00@gmail.com), Andrzej Grzywacz (hydrotaea@gmail.com)

Received 1 December 2023
Accepted 1 February 2024
Published 25 April 2024

Academic Editors Bradley Sinclair, Klaus-Dieter Klass

Citation: Walczak K, Pape T, Wallman JF, Szpila K, Grzywacz A (2024) To see the unseen: notes on the larval morphology and systematic position of *Achanthiptera* Rondani (Diptera: Muscidae). Arthropod Systematics & Phylogeny 82: 305–322. https://doi.org/10.3897/asp.82.e116703

Abstract

The muscid genus *Achanthiptera* Rondani (Diptera: Muscidae) was classified within its own subfamily Achanthipterinae for decades due to a misinterpretation of adult morphology. Conversely, the larval morphology suggested that *Achanthiptera* should be classified within Azeliinae, yet no formal changes were implemented based on this source of data. Using scanning electron microscopy (SEM) and confocal laser scanning microscopy (CLSM), we examined the larval morphology of *Ac. rohrelliformis* (Robineau-Desvoidy), *Potamia littoralis* Robineau-Desvoidy and *Australophyra rostrata* Robineau-Desvoidy. Despite the challenges posed by the poor condition of hundred-year-old museum specimens of *Ac. rohrelliformis* for light microscopy, CLSM examination yielded satisfactory results. Additionally, CLSM observations revealed peculiar modifications to the cephaloskeleton, including a dome-shaped (second instar) or spade-like (third instar) anterior rod attached to each mouthhook in *Ac. rohrelliformis* and *P. littoralis*. These structural modifications are likely to enhance the efficiency of food collecting by enlarging the surface of the mouthhooks. The results of our morphological analyses lead to the conclusion that larvae of *Au. rostrata* are facultative carnivores, while modified accessory oral sclerites in *Ac. rohrelliformis* and *P. littoralis* suggest a saprophagous feeding strategy. This study contributes new evidence that *Achanthiptera* is the sister taxon to *Potamia* Robineau-Desvoidy, and both are nested within the subfamily Azeliinae.

Key words

Achanthiptera rohrelliformis, anterior rod, confocal laser scanning microscopy, oral bar, saprophagy

1. Introduction

Achanthiptera rohrelliformis (Robineau-Desvoidy) is the sole representative of the muscid genus *Achanthiptera* Rondani. Most records and observations of this species are from the European part of the Palaearctic Region (Zielke 2018), but it has also been recorded from China (Shanxi), Siberia and Tajikistan (Skidmore 1985; Sorokina and Pont 2010). Since *Ac. rohrelliformis* is an uncommon species (Lobanov 1975; Bloxham 1982) with

short-lived adults (Skidmore 1985), information about its biology is scarce and found in only a handful of publications. Until now, adults of *Achanthiptera* have been noticed visiting colonies of aphids (Homoptera: Aphididae) (Cuny 1978), and females have been observed near vespid (Hymenoptera: Vespidae) nests where they lay eggs containing fully formed first-instar larvae, which hatch immediately after oviposition (Séguy 1923) and feed on decaying matter (Skidmore 1985). Larvae have been reported from nests of species of *Vespa* Linnaeus and *Vespula* Thomson (Hennig 1965; Bloxham 1978; Skidmore 1985), yet Lobanov (1975) also found them under moss on a drying swamp and in soil under decaying honey fungi *Armillaria* (Fr.) Staude. The fact that *Achanthiptera* larvae have been found in different substrates was overlooked, leading to a common belief that this genus is associated exclusively with social Hymenoptera (Skidmore 1985). Taking this into consideration, as well as the morphology of the third-instar cephaloskeleton, Skidmore (1985) concluded that larvae of *Achanthiptera* are trimorphic facultative carnivores, signifying the presence of three free-living larval instars.

The systematic position of *Achanthiptera* has long been a matter of great interest. *Achanthiptera* was assigned to the tribe Achanthipterini (Hennig 1955) and later to the tribe Phaoniini (Assis Fonseca 1968), in both cases of the paraphyletic subfamily Phaoniinae. Hennig (1965) concluded that *Achanthiptera* should be classified in its own subfamily based on his earlier observation (Hennig 1955) that a spiracle is retained in the female abdominal segment 6, distinguishing it from all other adult Muscidae, which lack spiracles distal to abdominal segment 5 (except *Cariocamyia* Snyder (Vockeroth 1972)). Later authors have widely accepted and implemented this classification over the years (Lobanov 1975; Michelsen 1977; Cuny 1978; Bloxham 1982; Pont 1986; Rognes 1986; de Carvalho 1989; Couri 2007; Fan 2008; Kutty et al. 2008). Also Skidmore (1985) adopted Hennig's classification, despite recognising the similarity in the biology and morphology of larvae of *Ac. rohrelliformis* with species from the subfamily Azeliinae (Lobanov 1975; Skidmore 1985). Later re-examination of *Ac. rohrelliformis* revealed, however, that Hennig's (1955, 1965) observation was a misinterpretation (Kutty et al. 2014), thereby rejecting the sole morphological support for the monospecific subfamily Achanthipterinae. Based on this observation and results of molecular phylogeny reconstruction in which *Ac. rohrelliformis* formed a sister group with *P. littoralis* Robineau-Desvoidy, the genus *Achanthiptera* was assigned to the subfamily Azeliinae (Kutty et al. 2014, fig. 2). The close relationship between *Achanthiptera* and *Potamia* has been confirmed in subsequent morphological (Jorge 2016) and molecular studies (Haseyama et al. 2015; Grzywacz et al. 2017), and these two genera appear to be closely related to *Australophyra* Malloch (Grzywacz et al. 2017).

Australophyra and *Potamia* are both small muscid genera. *Australophyra* is limited to only one species, *Au. rostrata* Robineau-Desvoidy, restricted to the Australotropical Region (Pont 1973; Savage and Wheeler 2004) and *Potamia* is represented by seven species (Evenhuis and Pape 2023). *Australophyra* has been considered for some time a synonym of *Ophyra* Robineau-Desvoidy (Hardy 1939; Sabrosky 1948; Hennig 1955) or *Hydrotaea* Robineau-Desvoidy (Pont 1989) or regarded as a subgenus of *Ophyra* (Emden 1965). Recently *Australophyra* was resurrected as a valid genus based on adult morphology by Savage and Wheeler (2004), which was later supported by molecular analyses (Grzywacz et al. 2017). *Australophyra rostrata*, the black carrion fly, has been frequently found on human cadavers (Archer et al. 2006; Dawson et al. 2020) and animal carrion (Archer and Elgar 2003a, 2003b; McIntosh et al. 2017), particularly in the advanced stage of decomposition (Fuller 1932; Pont 1973). As a tertiary agent of myiasis, its veterinary importance is negligible as larvae develop in contaminated wool rather than causing fly strike (Zumpt 1965). Fuller (1934) and Skidmore (1985) stated that larvae of *Au. rostrata* are primarily saprophagous, but ultimately, because they have been observed preying on blow fly larvae and conspecific larvae, Skidmore (1985) regarded them as trimorphic facultative carnivores. The genus *Potamia* is widespread in the Holarctic and present in the Neotropical and Oriental regions (Pont 1986; Barták and Roháček 2011). Adults of the most common *Potamia* species, *P. littoralis*, have been frequently collected on tree trunks, honeydew, flowers, and visiting aphid colonies (Cuny 1978; Skidmore 1985), as well as on human cadavers and animal carrion (Grzywacz et al. 2017). In turn, larvae have been found in human faeces, animal dung, rotten wood, fungi, nests of yellow jackets, hornets (Zimin 1948; Skidmore 1985) and various hole-nesting birds (Iwasa and Hori 1993; Iwasa et al. 1995). Skidmore (1985) considered *Potamia* larvae as trimorphic facultative carnivores, however Séguy (1923) and Iwasa et al. (1995) believed the larvae to be saprophages or coprophages since they were found in faecal matter and in nesting materials, rather than feeding on nestlings or their carrion.

Despite numerous changes in the tribal and subfamilial classification of the family Muscidae, *Potamia* (since Hennig (1955, 1965)) and *Australophyra* (since Malloch (1923, 1925)) have consistently been considered as closely related to *Hydrotaea*. Whenever muscid classifications were rearranged, these genera were classified together in a higher-level taxon and assigned to the subfamily Azeliinae (Hennig 1965; Lobanov 1965; Pont 1973), supported by the morphology of both immatures and adults (Hennig 1955, 1965; Skidmore 1985; Pont 1986; de Carvalho 1989; Savage and Wheeler 2004; Couri 2010; Jorge 2016; Michelsen 2022) as well as by molecular analyses (Kutty et al. 2010, 2014; Haseyama et al. 2015; Grzywacz et al. 2017, 2021; Walczak et al. 2023). However, the composition and relationships among the remaining species within Azeliinae have undergone numerous changes over the years. Currently, this subfamily includes 13 genera (Savage and Wheeler 2004; Grzywacz et al. 2021) represented by at least 400 species worldwide (Pont, unpublished). Although species of Azeliinae have been the subject of relatively frequent phylogenetic inferences based primarily

on adult morphology and molecular studies, the systematic position of some azeliines, such as *Azelia* Robineau-Desvoidy, remains questionable (Savage and Wheeler 2004; Kutty et al. 2014; Haseyama et al. 2015; Grzywacz et al. 2017, 2021). Comprehensive analysis of larval morphology has already proven highly informative for inferring phylogenetic relationships (Piwczyński et al. 2017; Grzywacz et al. 2021). Thus, generating detailed morphological documentation of immature stages from taxa of uncertain or questionable taxonomic position is highly desirable. Nevertheless, with the exception of *Hydrotaea*, for which some species have well-described and documented larval stages, immature stage morphology of the remaining Azeliinae is poorly known, e.g., *Drymeia* Meigen and *Thricops* Rondani, or remains unknown. Current knowledge of the morphology of the preimaginal stages of *Ac. rohrelliformis* (Lobanov 1975; Skidmore 1985) and *P. littoralis* (Zimin 1948; Skidmore 1985) is limited to the third larval instar. Due to the attention from forensic studies, more information can be found on the larvae of *Au. rostrata*. O'Flynn and Moorhouse (1980) produced line drawings and short descriptions of the first and second instars of *Au. rostrata*, allowing for their differentiation from other carrion-breeding larvae, whereas Fuller (1932), Skidmore (1985) and Zumpt (1965) documented the morphology of the third instar. Published data are often superficial, encompassing only a few selected features and frequently lacking detailed illustrations. By utilising museum material in morphological studies, researchers can gain a better understanding of the evolutionary history and relationships of different taxa, especially for taxa difficult to obtain (Buenaventura et al. 2021). The morphological examination of museum specimens, however, may face obstacles due to damage caused by the passage of time as well as inappropriate storage conditions, including overexposure to UV light. In this paper, taking advantage of extensive material of immature stages of *Achanthiptera* recently revealed in European museum collections, we evaluate the efficiency of confocal laser scanning microscopy (CLSM) in visualising UV-overexposed and more than 100-year-old museum material. To achieve this, we study and document in detail the second- and third-instar larvae of *Ac. rohrelliformis* and *P. littoralis* as well as the third-instar larva of *Au. rostrata* using light microscopy (LM), scanning electron microscopy (SEM) and CLSM. Based on the results, we reinvestigate the systematic relationships between *Ac. rohrelliformis* and other Muscidae.

2. Materials and methods

Larvae of *Ac. rohrelliformis* were obtained from the Natural History Museum (BMNH), London (UK), the Natural History Museum of Denmark (NHMD), University of Copenhagen, Copenhagen (Denmark) and the Museum für Naturkunde (ZMB), Leibniz Institute for Evolution and Biodiversity Science, Berlin (Germany). The museum material from BMNH and NHMD was preserved in ethanol, while samples from ZMB were dried and collapsed (due to evaporation of ethanol). After this was revealed, the material was re-preserved in ethanol. Procedures for obtaining *P. littoralis* larvae, including collection of gravid females during fieldwork and laboratory rearing and killing of larvae, followed the protocols described by Grzywacz et al. (2014). Briefly, adults of *P. littoralis* were attracted to baits (decomposed chicken liver) in Pławin (Poland) in 2013 and collected using an entomological net. Females were then transported to the laboratory in 2-mL Eppendorf tubes with air exchange provided by incaps punctures. In the laboratory, flies were transferred to plastic containers with a thin layer of wet sand and supplied with water, sugar and a small piece of chicken liver as an oviposition and feeding medium. Larvae of appropriate instars were transferred to a Petri dish and immersed in sub-boiling water (~97°C) for 60 s and then transferred to 70% ethanol. Larvae of *Au. rostrata* were collected from a human cadaver as part of a police investigation (Kuitpo Forest, South Australia). Soft forceps were used to collect the larvae, which were brought to the laboratory and preserved as described for *P. littoralis*. Larvae of *P. littoralis* and *Au. rostrata* are deposited in the Department of Ecology and Biogeography, Nicolaus Copernicus University in Toruń, Toruń, Poland (NCUT).

Third-instar larvae were prepared for SEM examination by cleaning with a fine brush, dehydration in 80.0%, 90.0% and 99.5% ethanol (EtOH) and critical-point-drying in carbon dioxide (CO_2) with an Autosamdri®-815, Series A critical-point-dryer (Tousimis Research Corp., Rockville, MD, U.S.A.). Larvae were then mounted on aluminium stubs with double-sided adhesive tape and coated with platinum for 140 s (20 nm of coating) using a JEOL JFC 2300HR high-resolution fine coater (JEOL Ltd., Tokyo, Japan). Scanning electron microscopy images were obtained with a JEOL scanning microscope (JSM-6335F; JEOL Ltd.).

CLSM observations were performed with a Leica TCS SP8 confocal laser scanning microscope (Leica Microsystems, Wetzlar, Germany). Larvae intended for CLSM analysis were prepared according to the protocol by Szpila et al. (2021). Second-instar larvae of *Ac. rohrelliformis* and *P. littoralis* were macerated by immersion in 10% potassium hydroxide (KOH) for 16 hours at room temperature. Third-instar larvae of *Ac. rohrelliformis* had faded due to exposure from UV light and, to avoid over-macerating, the material was macerated twice, initially for 12 hours and subsequently for an additional 5 hours after an assessment showed that the first maceration was insufficient due to large amounts of remaining soft tissue residues. Third-instar larvae of *P. littoralis* and *Au. rostrata* were macerated for 26 hours. Subsequently, all larvae were washed by placing them in 99.5% EtOH, transferred to a microscope slide with a drop of glycerine and covered with a coverslip. The acquisition steps were conducted in accordance with the protocol provided by Walczak et al. (2022). The autofluorescence signal of the cephaloskeleton was collected with two excitation wavelengths: 561 nm and 633 nm, as well as 488 nm in case of the mouthhooks of *Ac. rohrelliformis*. The microscope

Table 1. Abbreviations of morphological structures.

a1–7	abdominal segments 1–7	*mh*	mouthhook
abr	antennal basal ring	*mp*	maxillary palpus
acc	accessory stomal sclerites	*ns1–2*	additional sensillum coeloconicum 1–2
ad	anal division	*ob*	oral bar
an	antennal complex	*ol*	optic lobe
and	antennal dome	*or*	oral ridges
ao	anal opening	*p1–p7*	papillae 1–7
ap	anal plate	*pa*	post-anal papilla
aro	anterior rod	*paa*	para-anal papilla
as	anterior spiracle	*pb*	parastomal bar
asb	anterior spinose band	*pc*	pseudocephalon
bm	bubble membrane	*pp*	posterior projection
bs	basal sclerite	*pre*	pre-anal welt
cir	cirri	*ps*	posterior spiracle
cl	cleft	*r*	rami
cut	cutaneous teeth	*rp*	rectangular accessory process
db	dorsal bridge	*rs*	respiratory slit
dc	dorsal cornu	*sa*	sub-anal papilla
de	dorsal extension	*sb1–3*	sensillum basiconicum 1–3
ds	dental sclerite	*sc1–3*	sensillum coeloconicum 1–3
es	epistomal sclerite	*ss*	spiracular scar
ex	extra-anal papilla	*st*	spiracular tuft
is	intermediate sclerite	*sub*	suprabuccal teeth
ko	Keilin's organ	*t1–3*	thoracic segments 1–3
lcw	lateral creeping welt	*vb*	ventral bridge
ll	labial lobe	*vc*	ventral cornu
lo	labial organ	*vcw*	ventral creeping welt
lr	longitudinal ridges	*vo*	ventral organ
ls	labial sclerite	*vp*	vertical plate

slides were scanned with a 40x oil lens with a numerical aperture of 1.3 (N.A.=1.3). Following the acquisition of sequential images, maximum intensity projections (MIP) and 3D visualisation were built using LAS AF V3.3 and LAS X 3D Viewers (Leica Microsystems, Wetzlar, Germany), respectively.

Larval terminology follows Courtney et al. (2000) with a few modifications proposed by Szpila and Pape (2005). Family-specific structures follow the terminology of Skidmore (1985) with modifications proposed by Grzywacz (2013a) and Walczak et al. (2022). All abbreviations used in this study are listed in Table 1.

3. Results

3.1. Specimens examined

Achanthiptera rohrelliformis (Robineau-Desvoidy) (Figs 1A, B, 2A–F, 3A–G, 4A–I): 2 third-instar larvae, labelled: "C.27:1"; **BMNH** — 15 third-instar larvae, labelled: "April 1912 / Kryger / W. Lundbeck col."; **NHMD** — 35 second- and 27 third-instar larvae, labelled: "Berlin / Jungfernheide / 1909"; **ZMB** — 8 third-instar larvae, labelled: "Berlin / Wittenau / 1911"; **ZMB**

Potamia littoralis Robineau-Desvoidy (Figs 1C, D, 5A–C, E, G, 6A–I): 5 second- and 8 third-instar larvae, labelled: 21 Jul. 2013, Pławin, Poland, A. Grzywacz leg.; **NCUT**

Australophyra rostrata (Robineau-Desvoidy) (Figs 1E, 5D, F, H, 7A–I): 5 third-instar larvae, labelled: 1 Feb. 1995, Kuitpo Forest, South Australia, Australia, J. F. Wallman leg.; **NCUT**

3.2. General larval morphology

To avoid repetition, general morphology of all species is described jointly, and the species-specific details are highlighted in the following subsections. Due to the poor condition of the second-instar larva of *Ac. rohrelliformis*, it was only feasible to examine its cephaloskeleton using CLSM.

Pseudocephalon. Bilobate and equipped with paired antennal complex (*an*), maxillary palpus (*mp*) and ventral organ (*vo*) (Figs 3B, 6B, 7B). Functional mouth opening surrounded by facial mask consisting of numerous oral ridges (*or*) and a pair of labial lobes (*ll*) equipped apically with sensilla of the labial organ (*lo*) (Figs 3B, E, 6B, 7B). Anterior margin of the facial mask with a row of

cirri (*cir*). Antennal complex with conical antennal dome (*and*) situated on antennal basal ring (*abr*) (Figs 3C, 6B, 7B); the length of *and* half the height of *abr* (Figs 3C, 6B, 7B). The *mp* consists of three sensilla coeloconica (*sc*), three sensilla basiconica (*sb*), several small additional sensilla arranged in a tight cluster and two sensilla coeloconica of non-maxillary origin (*ns*) positioned laterodorsally (Figs 3D, 6C, 7C). The bulge-shaped *vo* equipped with four sensilla (Figs 3B, E, F, 6D, 7D) and placed at the anterior margin of *or* (Figs 3B, E, 6B, 7B).

Cephaloskeleton. Paired mouthhooks (*mh*), unpaired intermediate sclerite (*is*) and basal sclerite (*bs*) (Figs 1A–E).

Second instar with several well-sclerotized, ventrally directed suprabuccal teeth (*sub*) (Figs 2A, 5A) placed anterior to *mh*. The *mh* L-shaped in lateral view (Figs 1A, C, 2A, 5A) with slender base and distal parts symmetrical and closely appressed (Fig. 2B). Apical part of *mh* enveloped in the dome-shaped anterior rod (*aro*) (Figs 1A, C, 2A, B, 5A). Dental sclerite (*ds*) and irregular accessory stomal sclerites (*acc*) located below each *mh* (Figs 2A, 5A). Convex epistomal sclerite (*es*) and a pair of labial sclerites (*ls*) placed anteriorly between anterior arms of *is* (Figs 2A, 5A, B). Paired rod-like rami (*r*) lie freely between lateral arms of *is* (Figs 2B, 5B). Basal sclerite (*bs*) with paired vertical plates (*vp*), with dorsal (*dc*) and ventral cornua (*vc*) connected anteroventrally by strongly sclerotized ventral bridge (*vb*) (Figs 1A, C, 5A, B) and anterodorsally by tightly appressed horseshoe-shaped dorsal bridge (*db*) (Figs 1A, C, 5A). The *vp* broad, *dc* shorter than *vc* (Fig. 1A, C). Posterior parts of *dc* and *vc* poorly sclerotized, the latter with dorsal extension (*de*). Hypopharynx with distinctly developed longitudinal ridges.

Third instar with asymmetric, closely appressed *mh*, the left being shorter (Figs 2C, D, 5C, D). Distal parts curved ventrally (Figs 1B, D, E, 2C, D, 5C, D). Triangular *ds* and *acc* situated ventrally to base of each *mh* (Figs 2C, D, 5C, D). The *ds* connected with base of *mh* by slender, sclerotized hinge along anterodorsal margin (Figs 2C, D, 5C, D). Elongated and convex *es* and paired *ls* lie freely between anterior arms of *is* (Figs 2E, F, 5E, F). The *is* H-shaped in dorsal view (Figs 2F, 5E, F). Parastomal bar (*pb*) fused with dorsal margin of *is*, creating anterodorsal extension (Figs 2E, 5F, G, H). Paired well-sclerotized, rod-like rami (*r*) lie between arms of *is* (Figs 2F, 5E, F). The *bs* consists of paired, broad *vp* each with *dc* and *vc* (Fig. 1B, D, E). The *vp* connected anteroventrally by *vb* and anterodorsally by *db* (Figs 1B, D, E, 2F, 5E, F). Hypopharynx with longitudinal ridges.

Thoracic and abdominal segments. Anterior spinose band (*asb*) on first thoracic segment (*t1*) broad and complete (Figs 3A, B, 6A, B, 7A, B). Spines of *asb* colourless

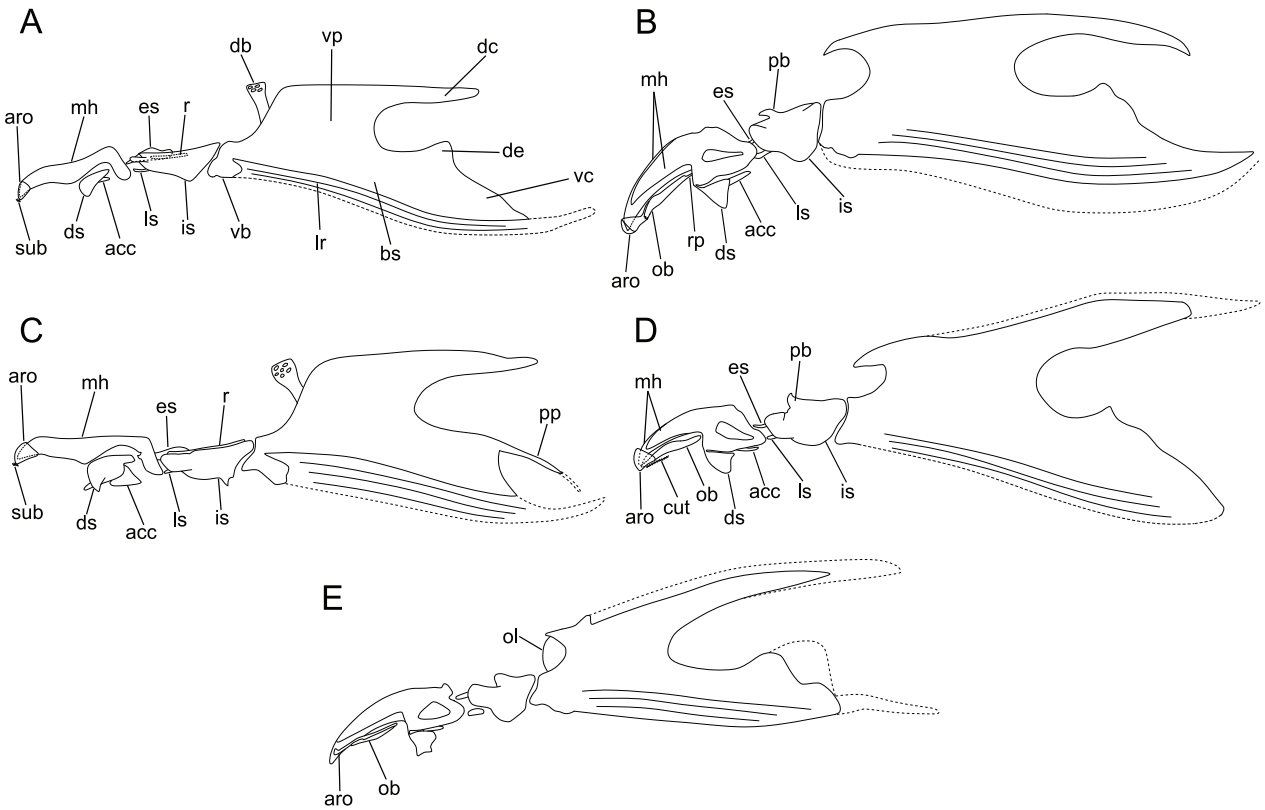

Figure 1. Details of cephaloskeleton in left-lateral views. **A** *Achanthiptera rohrelliformis*, second-instar larva. **B** *Achanthiptera rohrelliformis*, third-instar larva. **C** *Potamia littoralis*, second-instar larva. **D** *Potamia littoralis*, third-instar larva. **E** *Australophyra rostrata*, third-instar larva. — Abbreviations: *acc*, accessory stomal sclerites; *aro*, anterior rod; *bs*, basal sclerite; *cut*, cutaneous teeth; *db*, dorsal bridge; *dc*, dorsal cornu; *de*, dorsal extension; *ds*, dental sclerite; *es*, epistomal sclerite; *is*, intermediate sclerite; *lr*, longitudinal ridges in hypopharynx; *ls*, labial sclerite; *mh*, mouthhook; *ob*, oral bar; *ol*, optic lobe; *pb*, parastomal bar; *pp*, posterior projection; *r*, rami; *rp*, rectangular accessory process; *sub*, suprabuccal teeth; *vb*, ventral bridge; *vc*, ventral cornu; *vp*, ventral cornu.

and arranged densely in long rows, closely adjacent ventrally and slightly separated dorsally (Figs 3A, 6A, 7A). Anterior third of *t1* with transverse cleft (*cl*), followed ventrally by several rows of spines (Figs 3A, 6A, 7A). Each thoracic segment ventrally with a pair of trichoid sensilla of Keilin's organ (*ko*) (Figs 3B, 4B, 7A, E). Second (*t2*) and third (*t3*) thoracic and first abdominal (*a1*) segments in second instar with single short row of fine spines. Third instar with complete anterior spinose bands on *t2* and *t3* arranged in relatively short rows (Figs 3A, 6A, 7A). Abdominal segments (*a2–a7*) anteroventrally with creeping welts (*vcw*) and anal division (*ad*) with pre-anal welt (*pre*) (Figs 4C, I, 6F, I, 7F, I). Elliptical lateral creeping welts (*lcw*) present between abdominal segments, barely visible, never covered by spines (Fig. 7F). The posterolateral margin of *a1* with circular bubble membrane (*bm*) of many globules clustered together and level with the adjacent integument (Figs 4D, 6F, 7F). All spines of *asb* on *t1–t3* and *a1–a3*, as well as of *vcw* on *a2–a7* directed posteriorly (Figs 3A, B, G, 4A, C, 6A, B, F, 7A, B, F), while spines of *pre* point anteriorly (Figs 4I, 6I, 7I). Scars from muscle attachments strongly visible on surface of all thoracic and abdominal segments.

Anal division. Ventrally with anal opening (*ao*), porous anal plate (*ap*) and distinct anal papillae (Figs 4I, 6I, 7I). An unpaired post-anal papilla (*pa*) present directly posterior to *ao*. Paired sub-anal (*sa*), para-anal (*paa*) and extra-anal (*ex*) papillae shifted anteriorly relative to the *pa* (Figs 4I, 6I, 7I). Each *sa* with a sensillum basiconicum and two sensilla resembling sensilla ampullacea. Spiracular field with seven pairs of papillae (*p1–p7*) and a pair of posterior spiracles (*ps*) located centrally (Figs 4G, H, 6H, 7H). Each papilla composed of a sensillum plus the surrounding area. Papillae *p1*, *p3*, *p5* and *p7* with a sensillum basiconicum. Papillae *p2*, *p4* and *p6* indistinct, placed ventral to the spiracular field and equipped with a sensillum ampullaceum.

3.3. Specific morphology

3.3.1. Second instar: *Achanthiptera rohrelliformis*

Cephaloskeleton. Arched *ds*, *acc* and the pair of *r* weakly sclerotized (Fig. 2A, B).

3.3.2. Second instar: *Potamia littoralis*

Pseudocephalon. The *and* encircled with equidistantly spaced pores. The perimeter of the *mp* composed of two nearly circular folds. The *cir* angular and serrated. The *or* digitate along their entire length.

Cephaloskeleton. Base of *mh* with a hooked appendage on the ventral side (indicated by an asterisk in Fig. 5A). The *ds*, *acc* and a pair of *r* robust and strongly sclerotized (Fig. 5A, B). The *de* equipped with a sclerotized posterior projection (*pp*) directed ventrally (Fig. 1C).

Anal division. The *ao* surrounded by convex, W-shaped *ap*, which is anteriorly bounded by the *pre*, posteriorly by a row of conical spines. The *pa*, *sa* and *ex* bulge-like, *paa* flattened. Papillae *p1*, *p3*, *p5* and *p7* positioned level with adjacent integument. The *ps* slightly elevated and each *ps* bears two slightly sinuate and subparallel respiratory slits (*rs*), four branched spiracular tufts (*st*) and a median spiracular scar (*ss*).

3.3.3. Third instar: *Achanthiptera rohrelliformis*

Pseudocephalon. The perimeter of the *mp* composed of two nearly circular folds (Fig. 3B, D). The *or* serrated along entire length (Fig. 3A, B, E).

Cephaloskeleton. Left *mh* considerably shorter than right *mh* (Fig. 2C, D). Distal part of right *mh* massive, left one slender (Fig. 2C, D). Basal part of *mh* on right side joins with *ob* through a small rectangular accessory process (*rp*) (Fig. 2C). The *ob* serrated apically and parallel to the distal part of *mh* through entire length (Fig. 2C). A transformed *aro* embedded anteriorly to *ob* (Fig. 2C). The *aro* narrow at the base and strongly expanded apically. The apical part of *aro* covers the tip of right (and longer) *mh* (Fig. 2C, D). The irregular *ob* and short *aro* tightly appressed to *mh* (Fig. 2D, lateral view from left *mh*). The *dc* slender and slightly shorter than *vc*, which carries *de* (Fig. 1B).

Thoracic and abdominal segments. Spines of *asb* trapezoid with serrated posterior margin (Fig. 3B). The anterior spiracle (*as*) equipped with four or five lobes (Fig. 3A). Spines of anterior spinose bands on *t2* and *t3* of various shape from slightly pointed to blunt-ended (Fig. 3A, G). First three abdominal segments (*a1–a3*) with complete anterior spinose band of colourless, mostly blunt-ended spines that are arranged in short rows (Fig. 4A). In the middle of each *vcw* is a protuberance with at least two rows of conical spines surrounded by several rows of fine, single- and double-pointed spines (Fig. 4C). Anterior part of *pre* with small spines arranged in short rows similar to those of *vcw*, posterior part with irregularly arranged, more or less conical spines that are twice as large (Fig. 4I). Lateral creeping welts (hardly distinguishable) present posterolaterally on each abdominal segment.

Anal division. The *ao* surrounded by W-shaped *ap*, anteriorly limited by *pre* and posteriorly by bulge-shaped *pa* and *sa* (Fig. 4I). The *pa* covered with tiny spines and bigger than *sa*. Beyond each *sa* are paired, relatively flattened *paa* and *ex*, the latter larger than other anal papillae and covered with small spines (Fig. 4I). Anal papillae followed by several rows of tiny spines (Fig. 4I). Each of *p1*, *p3*, *p5* and *p7* in the form of a small integumental protuberance (Fig. 4G, H). The *ps* slightly elevated and relatively small, comparable in size to *p1* (Fig. 4H). Each *ps* with three straight *rs* in convergent arrangement, four branched *st* and *ss* in median position (Fig. 4E).

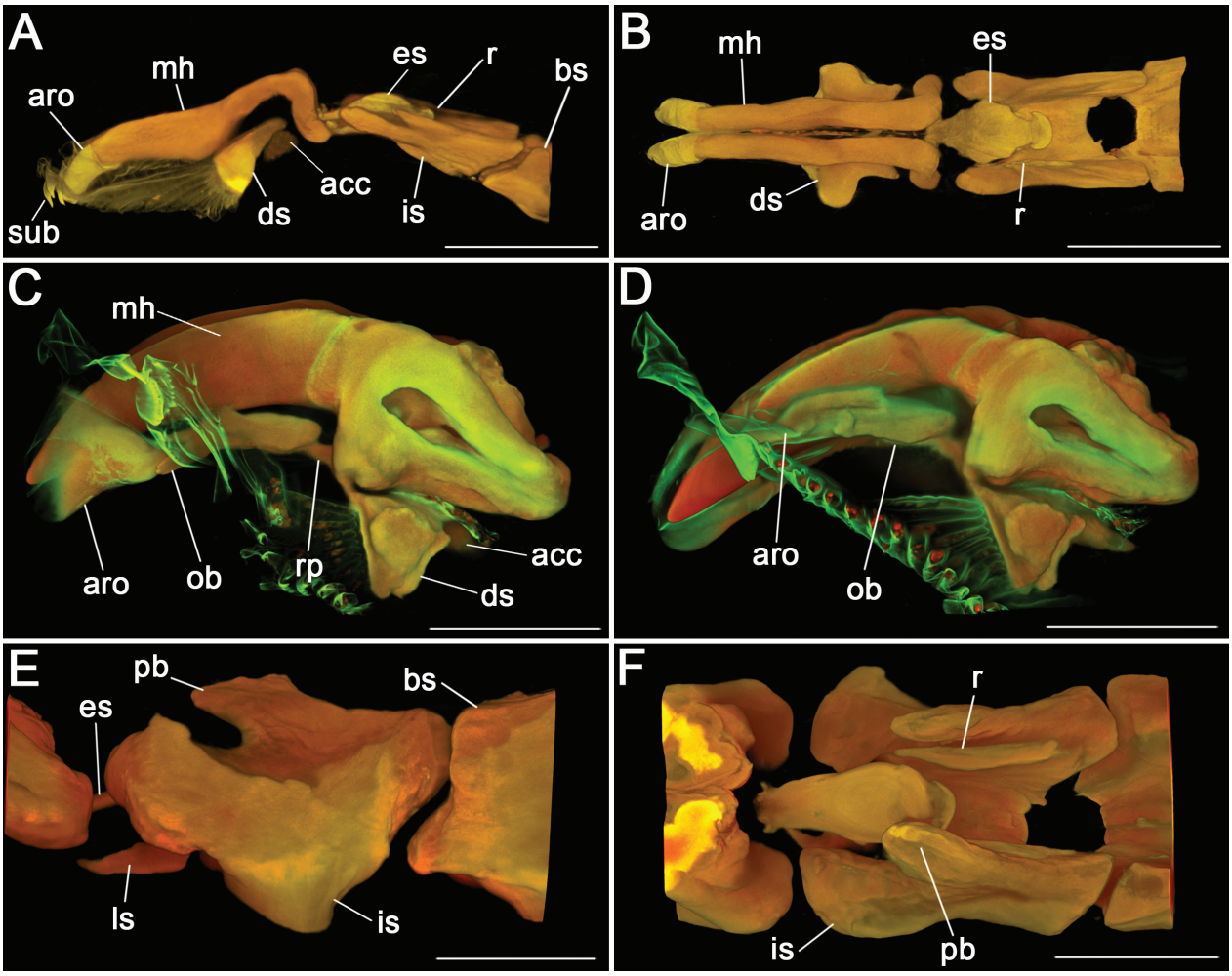

Figure 2. *Achanthiptera rohrelliformis*, cephaloskeleton of larvae II and III [CLSM]. **A** anterior end of cephaloskeleton of second-instar larva, lateral view. **B** mouthhooks and intermediate sclerite of second-instar larva, dorsal view. **C** mouthhooks of third-instar larva, lateral view of right mouthhook. **D** mouthhooks of third-instar larva, lateral view of left mouthhook. **E** intermediate sclerite of third-instar larva, lateral view. **F** intermediate sclerite of third-instar larva, dorsal view. — Abbreviations: *acc*, accessory stomal sclerites; *aro*, anterior rod; *bs*, basal sclerite; *ds*, dental sclerite; *es*, epistomal sclerite; *is*, intermediate sclerite; *ls*, labial sclerite; *mh*, mouthhook; *ob*, oral bar; *pb*, parastomal bar; *r*, rami; *rp*, rectangular accessory process; *sub*, suprabuccal teeth. Scale bars: 0.05 mm.

3.3.4. Third instar: *Potamia littoralis*

Pseudocephalon. The perimeter of the *mp* consists of an inner fold with four crescents and an outer circular fold (Fig. 6B, C). The *or* bluntly serrated along entire length (Fig. 6A, B). The *cir* trapezoid (Fig. 6B).

Cephaloskeleton. The *mh* asymmetrical with tip of *mh* covered by a transformed *aro* in right lateral view (Figs 1D, 5C). Right *aro* with narrow basal part tightly attached to *ob* and strongly expanded apical part in the form of an incomplete dome (Figs 1D, 5C). Two rows of minute cutaneous teeth (*cut*) ventral to the rod-like *ob* (Fig. 5C). The *ds* connected to base of *mh* through narrow, sclerotized hinge [ruptured in the examined specimen] (Fig. 5C). The *es* massive, convex in lateral view, elliptical in dorsal view, with two perforations located on anterolateral margin (Fig. 5E). A pair of rod-like *r* adheres ventrally to each arm of *is* (Fig. 5E). The *dc* slightly shorter and half the height of *vc*, the latter with well-developed *de* posterodorsally. The *vb* well-sclerotized, *db* less sclerotized and finely perforated (Fig. 1D).

Thoracic and abdominal segments. Spines of *asb* trapezoidal, mostly double- or triple-pointed (Fig. 6B, E). The *as* equipped with six lobes (Fig. 6A). Spines of anterior spinose bands on *t2* and *t3* single-pointed (Fig. 6A). Spines on abdominal segments limited to anterior margin only ventrally (Fig. 6F). The *a1* anteroventrally covered by short rows of small, colourless spines. Spines of *vcw* arranged in transverse rows separated in the middle by narrow strip. Spines of two inner rows relatively massive, somewhat hook-shaped, mostly single-pointed, adjacent short rows consist of tiny single- and double-pointed spines (Fig. 6F). The *pre* consists of three irregular rows of robust, conical spines and is preceded with one or two rows of fine spines (Fig. 6I). Lateral creeping welts barely visible but present on posterolateral part of each abdominal segment.

Anal division. The *ao* surrounded by convex, W-shaped *ap* (Fig. 6I). The *ap* anteriorly bound by *pre*, posteriorly

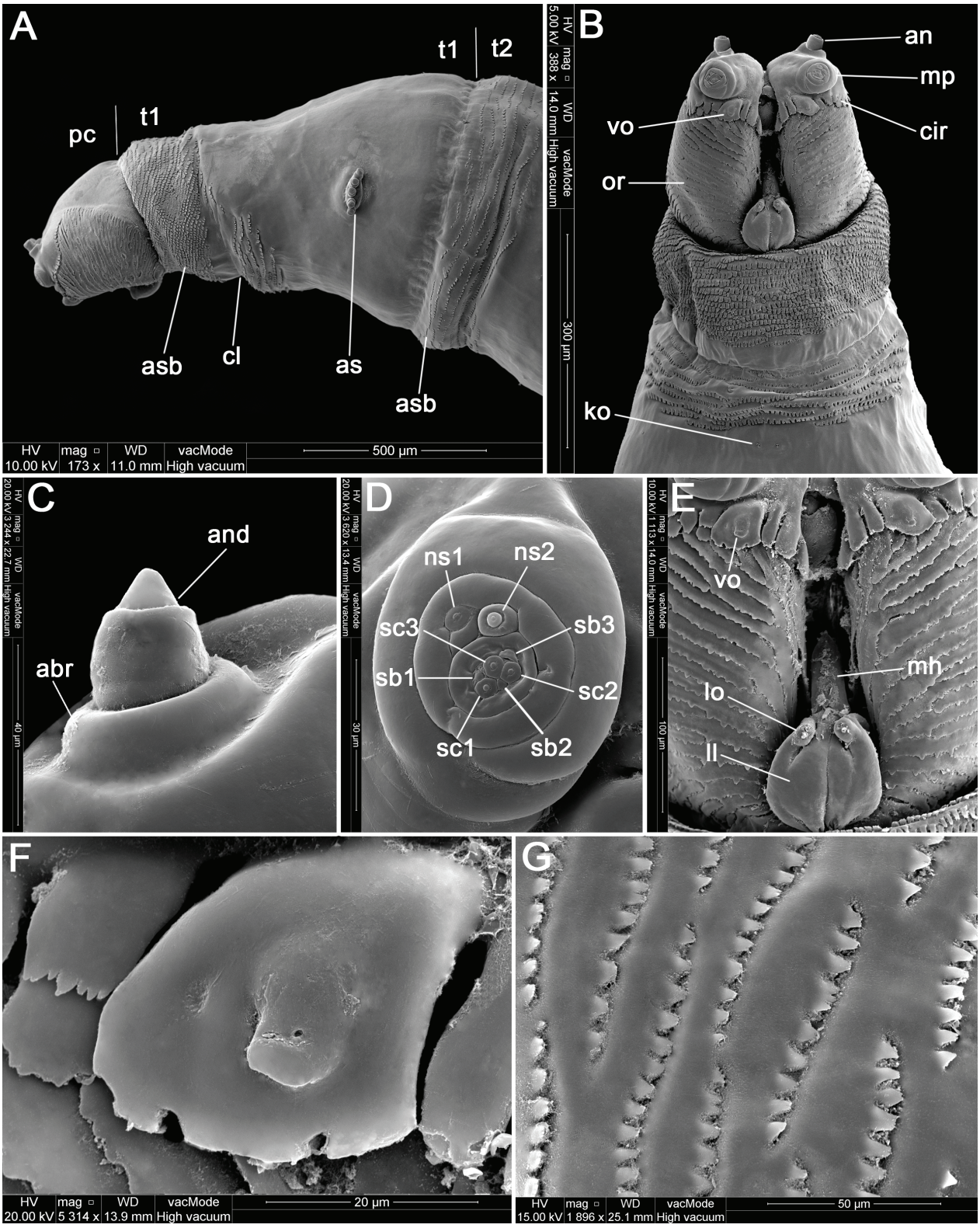

Figure 3. *Achanthiptera rohrelliformis*, pseudocephalon of third-instar larva [SEM]. **A** anterior end of body, lateral view. **B** anterior end of body, ventral view. **C** antennal complex. **D** maxillary palpus. **E** facial mask, ventral view. **F** ventral organ. **G** spines on first thoracic segment. — Abbreviations: *abr*, antennal basal ring; *an*, antennal complex; *and*, antennal dome; *as*, anterior spiracle; *asb*, anterior spinose band; *cir*, cirri; *cl*, cleft; *ko*, Keilin's organ; *ll*, labial lobe; *lo*, labial organ; *mh*, mouthhook; *mp*, maxillary palpus; *ns1–2*, first and second additional sensillum coeloconicum; *pc*, pseudocephalon; *or*, oral ridges; *sb1–3*, sensillum basiconicum 1–3; *sc1–3*, sensillum coeloconicum 1–3; *t1*, thoracic segment 1; *t2*, thoracic segment 2; *vo*, ventral organ.

by a row of spines similar in size and shape to those of the *pre* and further followed by several rows of small, conical spines (Fig. 6I). All anal papillae bulge-like, with *paa* being smallest and *ex* the largest. The *pa* covered with sharply pointed spines. Several irregularly scattered spines between *paa* and *ex*. The *p1*, *p3*, *p5* and *p7* po-

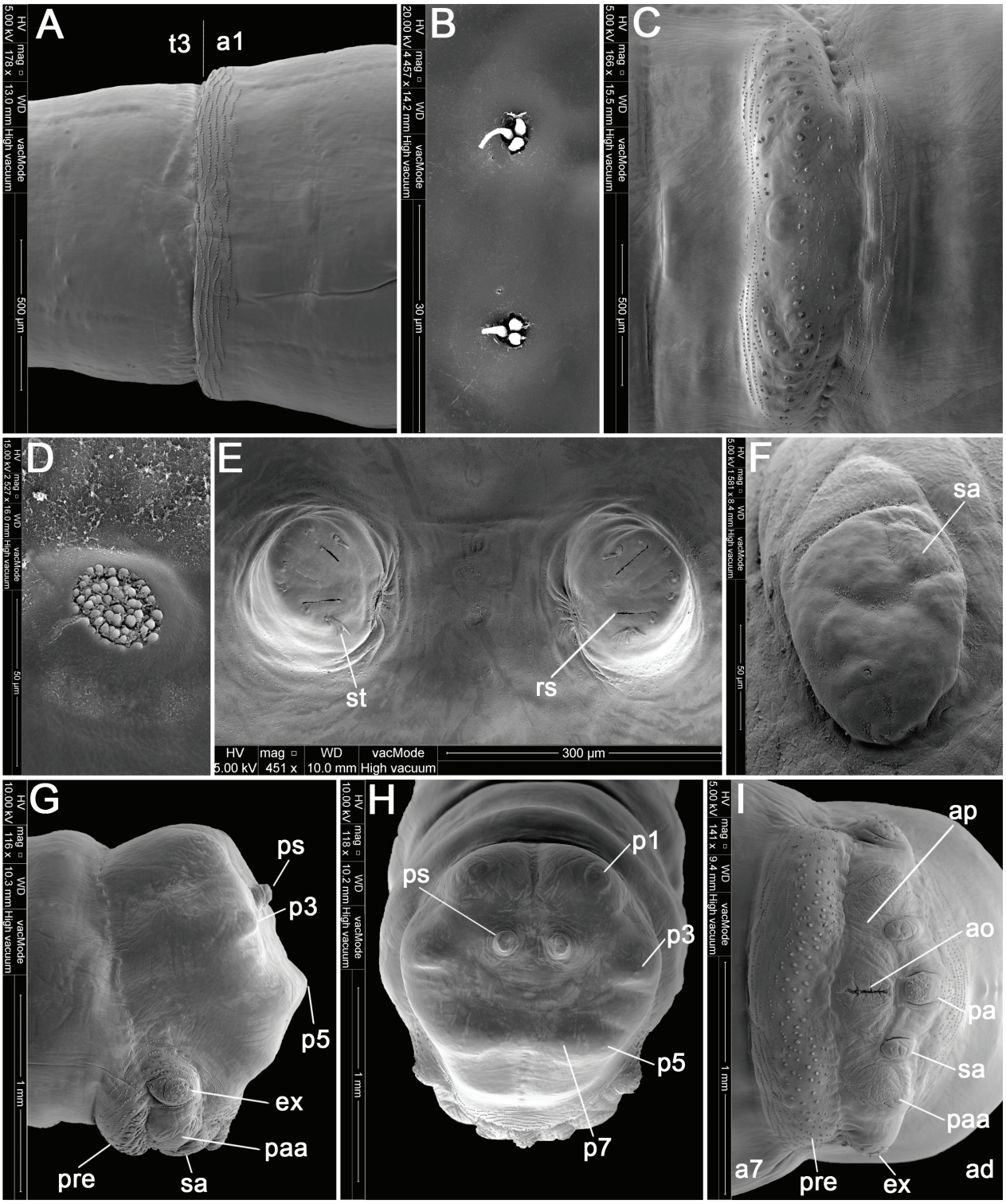

Figure 4. *Achanthiptera rohrelliformis*, thorax and abdomen of third-instar larva [SEM]. **A** third thoracic and first abdominal segments, lateral view, dorsal side up. **B** Keilin's organ on ventral side of third thoracic segment. **C** pre-anal welt on seventh abdominal segment, ventral view. **D** bubble membrane. **E** posterior spiracles. **F** sub-anal papilla. **G** posterior end of body, lateral view. **H** anal division, posterior view. **I** posterior end of body, ventral view. — Abbreviations: *a1*, abdominal segment 1; *a7*, abdominal segment 7; *ad*, anal division; *ao*, anal opening; *ap*, anal plate; *ex*, extra-anal papilla; *p1–p7*, papillae 1–7 surrounding spiracular field; *pa*, post-anal papilla; *paa*, para-anal papilla; *pre*, pre-anal welt; *ps*, posterior spiracle; *rs*, respiratory slit; *sa*, sub-anal papilla; *ss*, spiracular scar; *st*, spiracular tuft; *t3*, thoracic segment 3.

sitioned level with adjacent integument (Fig. 6H). The *ps* slightly elevated, each with three slightly sinuate and subparallel *rs*, four branched *st* and *ss* in median position (Fig. 6G).

3.3.5. Third instar: *Australophyra rostrata*

Pseudocephalon. The perimeter of the *mp* composed of three semi-circular folds (Fig. 7B, C). The *or* gently ser-

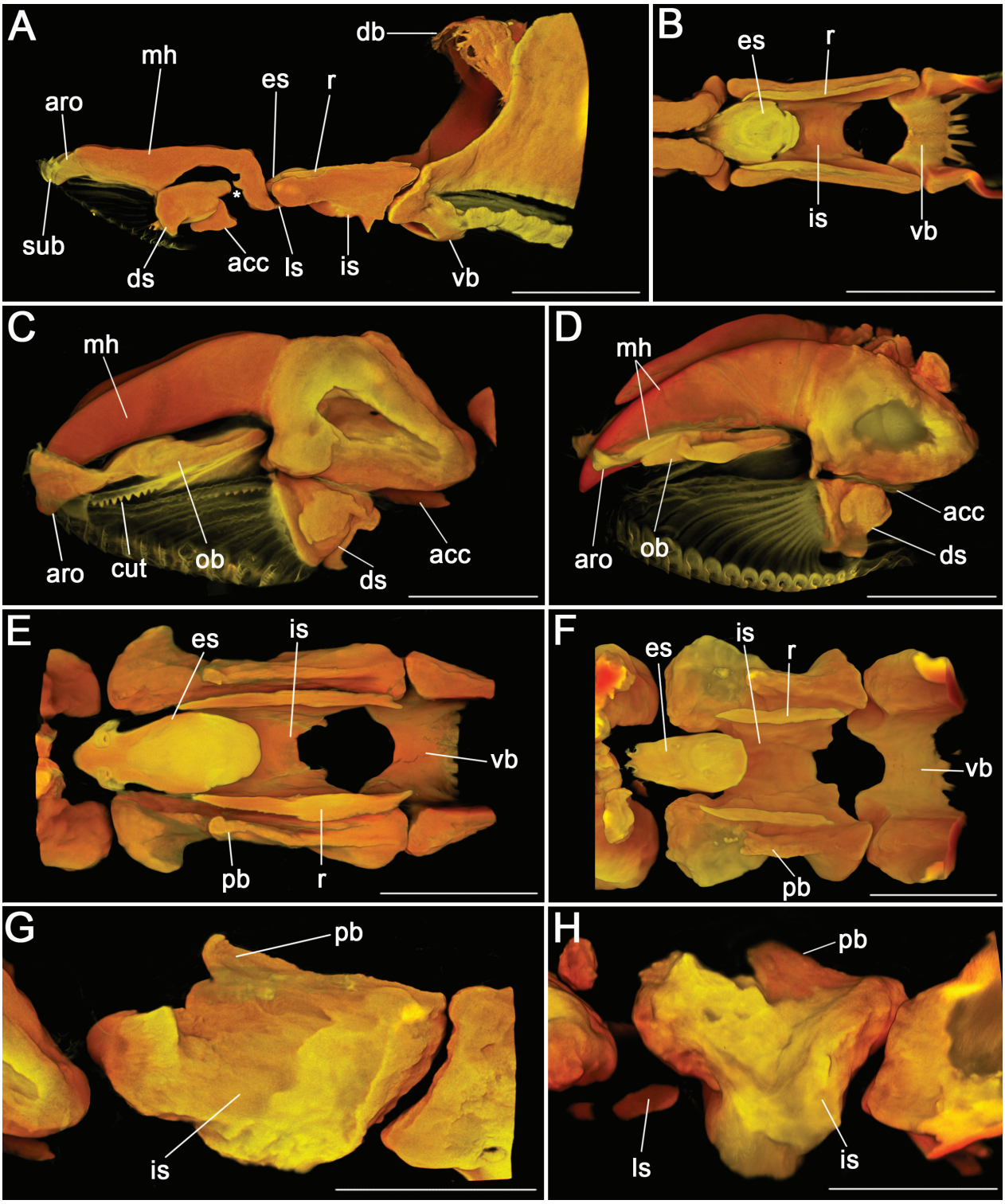

Figure 5. CLSM images of *Potamia littoralis* (A, B, C, E, G) and *Australophyra rostrata* (D, F, H). **A** anterior end of cephaloskeleton of second-instar larva with hooked appendage on ventral side of basal part of mouthhook (indicated by asterisk), left-lateral view. **B** intermediate sclerite and neighbouring elements of second-instar larva; dorsal view. **C** mouthhooks of third-instar larva, right-lateral view. **D** mouthhooks of third-instar larva, right-lateral view. **E** intermediate sclerite of third-instar larva; dorsal view. **F** intermediate sclerite and neighbouring elements of third-instar larva; dorsal view. **G** intermediate sclerite of third-instar larva; lateral view. **H** intermediate sclerite of third-instar larva; lateral view. — Abbreviations: *acc*, accessory stomal sclerite; *aro*, anterior rod; *cut*, cutaneous teeth; *db*, dorsal bridge; *ds*, dental sclerite; *es*, epistomal sclerite; *is*, intermediate sclerite; *ls*, labial sclerite; *mh*, mouthhook; *ob*, oral bar; *pb*, parastomal bar; *r*, rami; *sub*, suprabuccal teeth; *vb*, ventral bridge. Scale bars: 0.05 mm.

rated. The *vo* in the form of an irregularly rounded bulge in the cuticle (Fig. 7B, D). The *cir* only visible in lateral view (Fig. 7A).

Cephaloskeleton. The *ob* rod-like and not connected to base of asymmetrical *mh* (Fig. 5D). The *aro* toothed anteriorly and the elongated basal part tightly appressed to an-

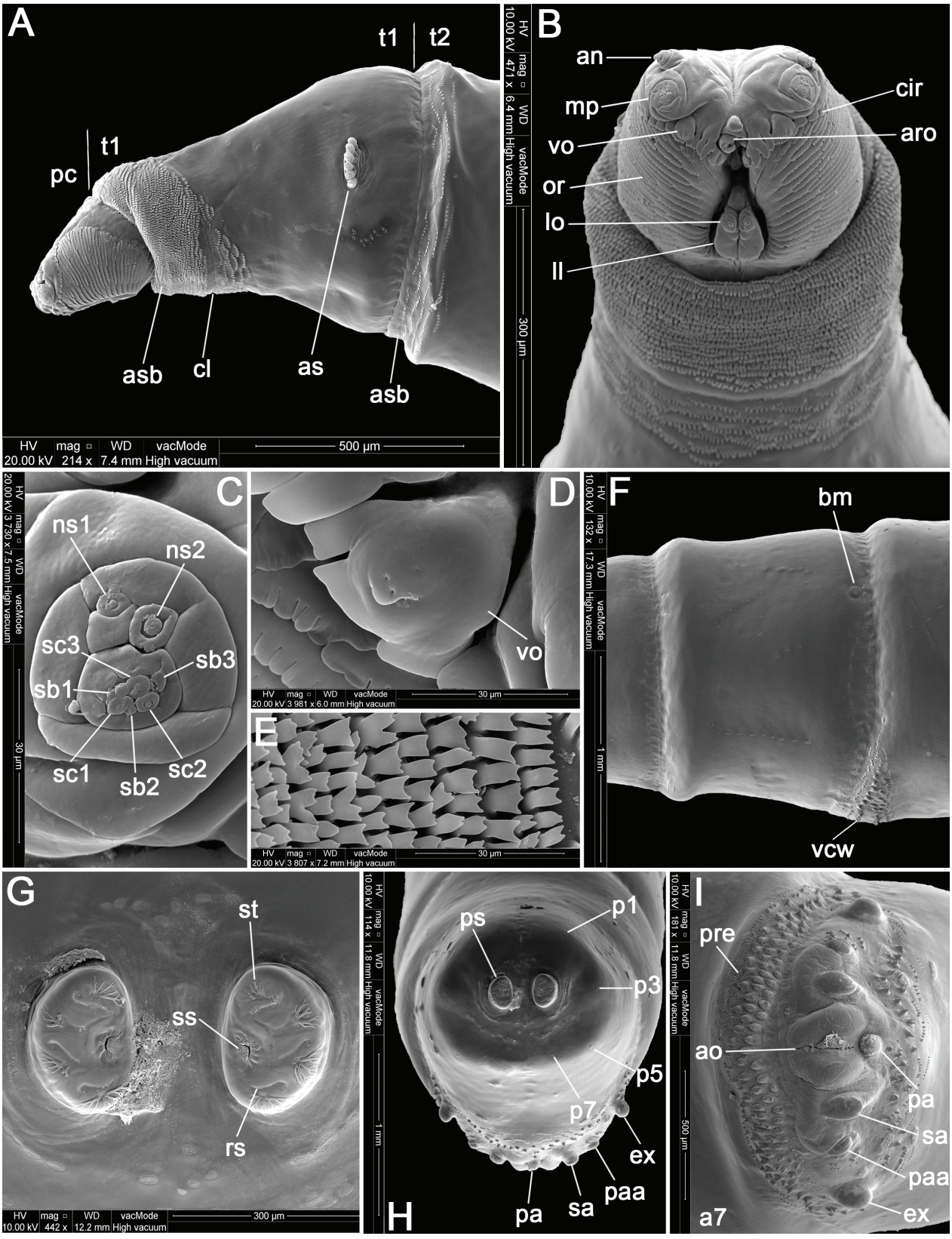

Figure 6. *Potamia littoralis*, pseudocephalon, thorax and abdomen of third-instar larva [SEM]. **A** anterior end of body, lateral view. **B** anterior end of body, ventral view. **C** maxillary palpus. **D** ventral organ. **E** spines on first thoracic segment. **F** first abdominal segment, lateral view, dorsal side up. **G** posterior spiracles. **H** anal division, posterior view. **I** posterior end of body, ventral view. — Abbreviations: *a7*, abdominal segment 7; *an*, antennal complex; *ao*, anal opening; *aro*, anterior rod; *as*, anterior spiracle; *asb*, anterior spinose band; *bm*, bubble membrane; *cir*, cirri; *cl*, cleft; *ex*, extra-anal papilla; *ll*, labial lobe; *lo*, labial organ; *mp*, maxillary palpus; *ns1–2*, first and second additional sensillum coeloconicum; *or*, oral ridges; *p1–p7*, papillae 1–7 surrounding spiracular field; *pa*, post-anal papilla; *paa*, para-anal papilla; *pc*, pseudocephalon; *pre*, pre-anal welt; *ps*, posterior spiracle; *rs*, respiratory slit; *sa*, sub-anal papilla; *sb1–3*, sensillum basiconicum 1–3; *sc1–3*, sensillum coeloconicum 1–3; *ss*, spiracular scar; *st*, spiracular tuft; *t1*, thoracic segment 1; *t2*, thoracic segment 2; *vcw*, ventral creeping welt; *vo*, ventral organ.

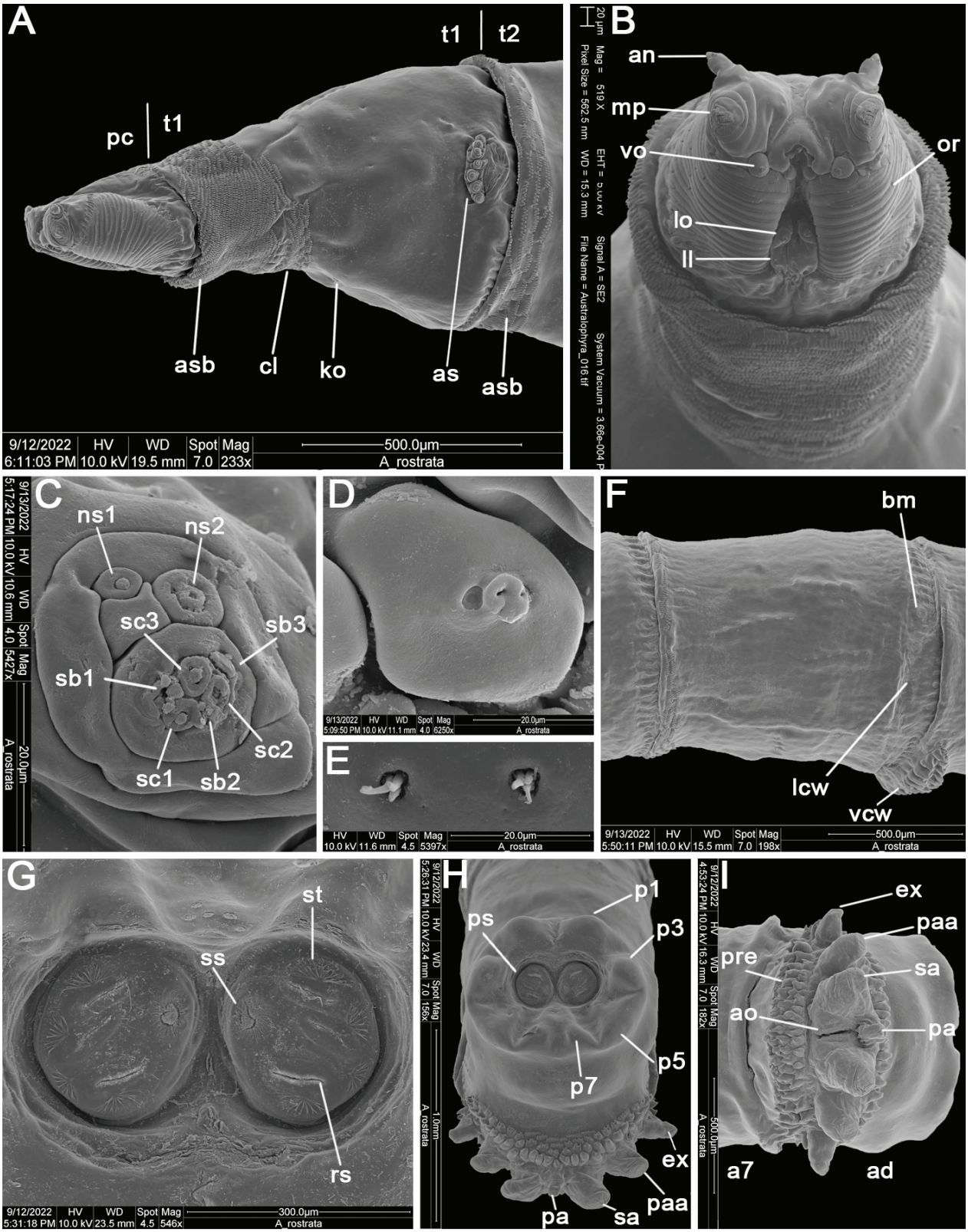

Figure 7. *Australophyra rostrata*, pseudocephalon, thorax and abdomen of third-instar larva [SEM]. **A** anterior end of body, lateral view. **B** anterior end of body, ventral view. **C** maxillary palpus. **D** ventral organ. **E** Keilin's organ on ventral side of third thoracic segment. **F** first abdominal segment, lateral view, dorsal side up. **G** posterior spiracles. **H** anal division, posterior view. **I** posterior end of body, ventral view. — Abbreviations: *a7*, abdominal segment 7; *ad*, anal division; *an*, antennal complex; *ao*, anal opening; *as*, anterior spiracle; *asb*, anterior spinose band; *bm*, bubble membrane; *cir*, cirri; *cl*, cleft; *ex*, extra-anal papilla; *ko*, Keilin's organ; *lcw*, lateral creeping welt; *ll*, labial lobe; *lo*, labial organ; *mp*, maxillary palpus; *ns1–2*, first and second additional sensillum coeloconicum; *or*, oral ridges; *p1–p7*, papillae 1–7 surrounding spiracular field; *pa*, post-anal papilla; paa, para-anal papilla; *pc*, pseudocephalon; pre, pre-anal welt; *ps*, posterior spiracle; *rs*, respiratory slit; *sa*, sub-anal papilla; *sb1–3*, sensillum basiconicum 1–3; *sc1–3*, sensillum coeloconicum 1–3; *ss*, spiracular scar; *st*, spiracular tuft; *t1*, thoracic segment 1; *t2*, thoracic segment 2; *vcw*, ventral creeping welt; *vo*, ventral organ.

terodorsal margin of *ob* (Figs 1E, 5D). Each *aro* slightly curved, forming an incomplete arch in dorsal view. The *is* relatively short (Figs 1E, 5F). Optic lobe (*ol*) present and weakly sclerotized (Fig. 1E). The *bs* is the least sclerotized part of the cephaloskeleton. The *dc* and *vc* of similar length (Fig. 1E). The *dc* slender, and *vc* twice as wide as *dc* and with weakly sclerotized *de* (Fig. 1E).

Thoracic and abdominal segments. Spines of *asb* slender and single-pointed, occasionally double-pointed (Fig. 7B). The *as* with seven to eight lobes (Fig. 7A). Spines of anterior spinose bands on *t2* and *t3* single- or double-pointed (Fig. 7A). The *a1* with *asb* incomplete laterally, ventrally with more rows of spines than dorsally (Fig. 7F). Spines of *asb* colourless and single-pointed, arranged in short rows. Spines of *vcw* relatively robust, conical and blunt-tipped, arranged in two transverse rows separated in middle by narrow strip and followed by row of smaller spines (Fig. 7F). The *pre* consists of three irregular rows of robust and conical spines that are preceded by one row of single-pointed spines (Fig. 7I). A transverse crevice present ventrally in middle part of segments *a1–a7*. A lateral creeping welt is distinctly developed posterolaterally on each abdominal segment.

Anal division. The *ap* almost entirely covered with massive anal papillae (Fig. 7I). Anterior margin of *ap* covered by the *pre*, posterior margin covered by broad strip of spines equal to those of the *pre*. All anal papillae enlarged and conical, together resembling a crown in dorsal and ventral view (Fig. 7H). Paired *sa*, *paa* and *ex* of similar size (Fig. 7I). The *p1*, *p3*, *p5* and *p7* form distinct bulges (Fig. 7H). The *ps* placed slightly below the surface of spiracular field (Fig. 7G, H), with three subparallel and slightly sinuous *rs*, four branched *st* and *ss* placed submedially (Fig. 7G, H).

4. Discussion

4.1. Systematic position of *Ac. rohrelliformis*

Phylogenetic implications based on larval morphology have been discussed for Muscidae by several authors (Roback 1951; Schumann 1954; Ferrar 1979; Skidmore 1985), and, among all larval structures, the cephaloskeleton has been identified as of particular importance. For instance, having observed a striking resemblance of the cephaloskeleton, including the shape and arrangement of sclerites between the larvae of *P. littoralis* and *Hydrotaea dentipes* (Fabricius), Hennig (1965) ultimately concluded that *Potamia* was more closely related to *Hydrotaea* than to *Phaonia* Robineau-Desvoidy. The asymmetry of the mouthhooks in the third-instar larva supports the placement of *Achanthiptera* as well as *Potamia* and *Australophyra* within the Azeliinae + Muscinae clade (Grzywacz et al. 2021). All species examined in this study are nested within the subfamily Azeliinae and have larvae closely resembling those azeliines for which descriptions and drawings are available. Similarities in general morphology and in the details of the cephaloskeleton and anal division with the *dentipes*-group within *Hydrotaea* are particularly compelling (Skidmore 1985; Grzywacz et al. 2014). Shared features are the shape of the anal division: angular outline of the segment in lateral view, spiracular field directed posterodorsally often with dorsal-most part of *ad* distinctly above the level of the dorsal surface of preceding abdominal segments, a W-shaped anal plate with all anal papillae well developed, mostly bulge-like, as well as posterior spiracles with straight to sinuate respiratory slits in a parallel to radiate arrangement (Skidmore 1985; Grzywacz 2013b; Grzywacz et al. 2014). In Muscinae, the spiracular field is directed posteriorly and the dorsal surface of the segment is not above the level of preceding abdominal segments, the anal plate is either small to enlarged, with partially reduced anal papillae, while the slits of the posterior spiracles are serpentine to torturous and arranged in a peripheral to encircling configuration (Skidmore 1985; Grzywacz 2013a). As for the differences in the cephaloskeleton, Azeliinae larvae usually possess well-developed accessory oral sclerites, while in larvae of the Muscinae these are absent or reduced (Skidmore 1985; Grzywacz 2013b; Grzywacz et al. 2014). In addition, the intermediate sclerite of Azeliinae is equipped with a visible anterodorsal extension derived from the reduced parastomal bar, while in Muscinae this sclerite is short and robust, and its dorsal surface is strongly modified (Fig. 8E, F).

4.2. Comparative morphology

Our results provide the first description of the morphology of the second-instar larva of *Ac. rohrelliformis* and *P. littoralis*. The species exhibit numerous similarities in their cephaloskeletons. Notably, the presence of a dome-shaped anterior rod closely attached to each mouthhook differentiates them from other muscid species. CLSM images revealed that each rod envelops the tips of the mouthhooks and further extends forward in relation to them. To the best of our knowledge, this specific shape of the anterior rod has not been documented previously and its function remains uncertain. Although previous studies have provided relatively detailed descriptions of spinulation pattern, arrangement of anal papillae and shape of posterior spiracles in the third-instar larva of *Ac. rohrelliformis*, *P. littoralis* and *Au. rostrata*, details of the cephaloskeleton have either been briefly described or not described at all. Illustrations of the third-instar larval body, the cephaloskeleton and the posterior spiracles were provided by Lobanov (1975) for *Ac. rohrelliformis*, by Zimin (1948) for *P. littoralis*, by Fuller (1932) and Zumpt (1965) for *Au. rostrata* and by Skidmore (1985) for all three species. Examination of these figures reveals that the authors observed all sclerites recognised in this study, except for the epistomal sclerite, parastomal bars, a pair of labial sclerites and a pair of rami in all exam-

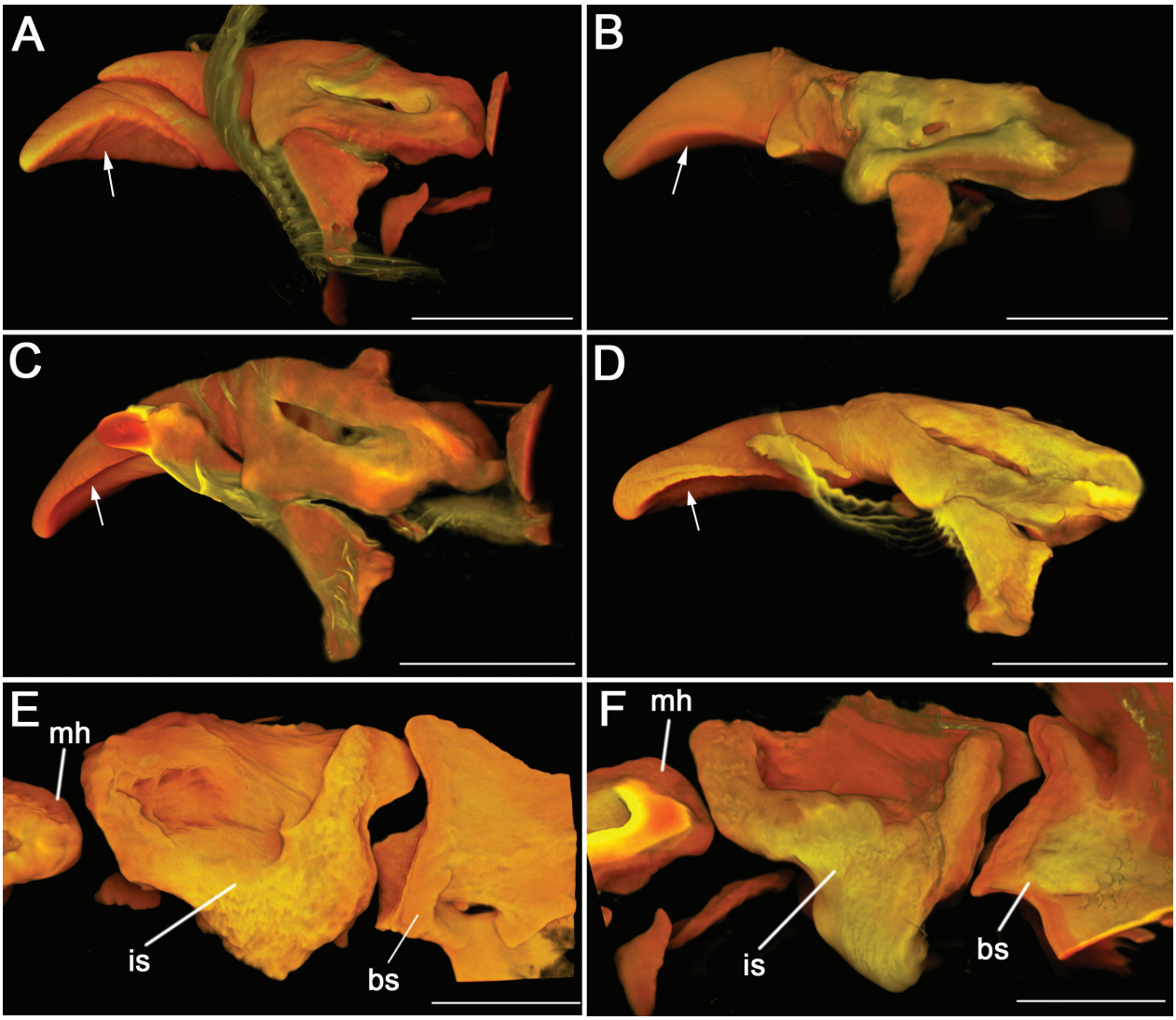

Figure 8. CLSM images of mouthhook of third-instar larvae of some representatives of *Musca*, *Stomoxys* and *Neomyia*. Expanded apical part of mouthhook assists coprophagous and saprophagous species to more efficiently collect food mass (A–D). **A** *Musca conducens* Walker, left-ventrolateral view. **B** *Stomoxys calcitrans* (Linnaeus), left-ventrolateral view. **C** *Neomyia gavisa* (Walker), right-ventrolateral view. **D** *Neomyia lauta* (Wiedemann), right-ventrolateral view. **E** intermediate sclerite of *N. lauta*, lateral view. **F** intermediate sclerite of *M. conducens*, lateral view. — Abbreviations: *bs*, basal sclerite; *is*, intermediate sclerite; *mh*, mouthhook. Scale bars: 0.05 mm.

ined species as well as the rectangular accessory process in *Ac. rohrelliformis*. Additionally, CLSM revealed that the dental sclerite in all examined species is connected to the base of the mouthhook by a narrow, sclerotized hinge. Skidmore (1985) noted that the intermediate sclerite of *Ac. rohrelliformis*, *P. littoralis* and *Au. rostrata* is equipped with a "very strong acute dorsal tooth", which corresponds to the location of the parastomal bar that has fused with the dorsal edge of the intermediate sclerite (Walczak et al. 2022). Despite the long-standing belief that the absence of a parastomal bar was considered a distinctive feature of the family Muscidae (Schumann 1954; Ferrar 1979; Skidmore 1985), recent evidence has demonstrated its presence in reduced form in muscid species (Walczak et al. 2022, 2023). Most importantly, all authors correctly observed the presence of additional sclerites below the apical part of the mouthhooks, however they did not recognise the asymmetry of the oral bars and anterior rods in *Ac. rohrelliformis*, as well as the peculiar shape of anterior rods in both *Ac. rohrelliformis* and *P. littoralis*. The right mouthhook in *Ac. rohrelliformis* is fused basally to a serrated oral bar through a rectangular accessory process, while its apical part is closely attached to a spade-like anterior rod. Below the left mouthhook, these structures are reduced, irregular and unconnected to the base of the mouthhook. Although asymmetry of the mouthhooks is a feature shared by all species in the subfamily Azeliinae (Grzywacz et al. 2021), the pronounced asymmetry of the accessory oral sclerites documented in this study has not been reported previously. While the mouthhooks and accessory oral sclerites do not exhibit such pronounced asymmetry in *P. littoralis*, they do possess comparably well-developed accessory oral sclerites as observed in *Ac. rohrelliformis*. This is in comparison with Skidmore (1985), who misinterpreted the anterior rod and oral bar in *P. littoralis* as

"very slender, short and weak". A similar inconsistency exists in the description of the morphology of *P. scabra* (Giglio-Tos). Skidmore (1985) mentioned the absence of accessory oral sclerites in this species, misinterpreting the line drawings presented by Calhoun et al. (1956), and thus considering *P. scabra* a sole representative of Azelinae devoid of accessory oral sclerites. A re-examination of fig. 3 in Calhoun et al. (1956) revealed that the third instar of *P. scabra* has accessory oral sclerites that are as well-developed or even more strongly developed than in *P. littoralis*. Similarly to *Ac. rohrelliformis*, the oral bar of *P. scabra* closely adjoins the basal part, and the anterior rod adjoins the apical part of the mouthhook. All aforementioned morphological structures, in particular the shape of accessory oral sclerites, and the connection between them, might have been overlooked by previous authors due to the limitations of light microscopy techniques. On the other hand, this might also have resulted from the process of microscopical preparation itself. This study revealed how maceration time in potassium hydroxide may critically impact the visibility of fine sclerites, making them nearly invisible. Individually adjusted maceration time is therefore strongly recommended for each specimen under study. Furthermore, Skidmore's cephaloskeletons of *Ac. rohrelliformis* and *P. littoralis* were dissected from puparia, which could have caused the displacement or rupture of small, weakly sclerotized morphological structures.

4.3. Functional morphology and notes on larval feeding strategy

The function of the modified anterior rods in *Ac. rohrelliformis* and *P. littoralis* remains ambiguous, and further investigation of larval biology would be necessary to unravel its significance. Keilin (1917) demonstrated a close relationship between larval feeding habits and the presence/absence and shape of cephaloskeletal elements, which was later refined by other authors (Keilin and Tate 1930; Thomson 1937; Roberts 1971; Ferrar 1979; Skidmore 1985). Based on the presence of additional oral sclerites and following the conclusions of previous authors, larvae of *Achanthiptera*, *Australophyra* and *Potamia* should be considered facultative carnivores. This larval feeding strategy is particularly indicated by relatively blunt-tipped mouthhooks, well-developed accessory oral sclerites composed of oral bars and anterior rods and well visible longitudinal ventral pharyngeal ridges. Accessory oral sclerites are known to play a vital role in facilitating the movement of mouthhooks when piercing the cuticle of the prey (Roberts 1971). When the mouthhooks are flexed downwards, the oral bars emerge from the functional mouth opening being held in place by the anterior rods to grip the cuticle of potential prey, as shown in fig. 5H in Grzywacz et al. (2014) (Roberts 1971; Skidmore 1973). While accessory oral sclerites in *Au. rostrata* resemble those of the majority of species within the genus *Hydrotaea* (Grzywacz et al. 2014), their modified shape in *Achanthiptera* and *Potamia* seems unlikely to support this function. It is therefore proposed here that the modified anterior rods in the second- and third-instar larvae of both *Achanthiptera* and *Potamia*, in conjunction with the mouthhooks, increase the surface area for collecting food mass. A similar modification for increasing the surface area of the mouthhooks for shovelling liquefied food has already been reported in some saprophagous and coprophagous species within the subfamily Muscinae. For example, species of *Musca* Linnaeus, *Neomyia* Walker and *Stomoxys* Geoffroy are known to have a laterally expanded apical part of the mouthhook (Fig. 8A–D), enabling more efficient collection of food mass (Ferrar 1979; Skidmore 1985). In *Atherigona* Rondani, in turn, a distinct modification of accessory oral sclerites is well known, reflecting the adaptive transition from facultative carnivory (e.g. *At. culicivora* Kovac, Pont and Deeming and *At. orientalis* Schiner) to phytophagy (e.g. *At. reversura* Villeneuve) (Skidmore 1985; Grzywacz and Pape 2013, 2014; Kovac et al. 2023). In the subgenus *Atherigona* s. str., the massively enlarged oral bar and the reduced mouthhook are fused, thereby functioning as a single structure. As a result, lateral movement is inhibited, and the fused sclerites functionally resemble the broadened mouthhooks of phytophagous Anthomyiidae (Roberts 1971; Ferrar 1987).

In summary, based on the current study and literature data, the larval instars of *Au. rostrata* are considered facultative carnivores, while strong asymmetry of mouthhooks and modified accessory oral sclerites in *Ac. rohrelliformis* indicate a saprophagous lifestyle. The larval morphology of the second and third instars of *P. littoralis* closely corresponds to that of *Ac. rohrelliformis*, the only difference being that in *P. littoralis* both oral bars lie freely. Nonetheless, considering similar modifications of accessory oral sclerites, we assume that both *P. littoralis* and *P. scabra* are saprophages, although this requires corroboration, such as through observations from rearing experiments.

5. Declarations

Funding statement. This research was supported by the National Science Centre of Poland (grant no. 2019/33/B/NZ8/02316 to AG) and the SYNTHESYS+ Projects http://www.synthesys.info/, which are financed by the European Community Research Infrastructure Action under the FP7 Integrating Activities Programme (grants nos. DE-TAF-3859, DK-TAF-3856, GB-TAF-3301 and GB-TAF-125 to AG and KW).

CRediT authorship contribution statement. Kinga Walczak: Conceptualization, Methodology, Investigation, Writing – Original draft, Writing – Review and Editing, Visualization. **Thomas Pape:** Resources, Writing – Review and Editing. **James F. Wallman:** Resources, Writing – Review and Editing. **Krzysztof Szpila:** Resources, Writing – Review and Editing. **Andrzej Grzywacz:** Conceptualization, Methodology, Writing – Review and Editing, Visualization, Funding Acquisition.

Declaration of Competing Interests. The authors have declared no competing interests.

6. Acknowledgements

We express our appreciation to Dr Joachim Ziegler (Museum für Naturkunde Leibniz-Institut für Evolutions- und Biodiversitätsforschung, Berlin, Germany), Mr Jaime A. Florez Fernandez (Australian National Insect Collection, CSIRO Ecosystem Sciences, Canberra, Australia) and Dr David K. Yeates (Australian National Insect Collection, CSIRO Ecosystem Sciences, Canberra, Australia) for help in obtaining material.

7. References

Archer MS, Elgar MA (2003a) Effects of decomposition on carcass attendance in a guild of carrion-breeding flies. Medical and Veterinary Entomology 17: 263–271. https://doi.org/10.1046/j.1365-2915.2003.00430.x

Archer MS, Elgar MA (2003b) Yearly activity patterns in southern Victoria (Australia) of seasonally active carrion insects. Forensic Science International 132: 173–176. https://doi.org/10.1016/S0379-0738(03)00034-3

Archer MS, Elgar MA, Briggs CA, Ranson DL (2006) Fly pupae and puparia as potential contaminants of forensic entomology samples from sites of body discovery. International Journal of Legal Medicine 120: 364–368. https://doi.org/10.1007/s00414-005-0046-x

Assis Fonseca ECM d' (1968) Diptera Cyclorrhapha Calyptrata Section (b) Muscidae. Handbooks for the Identification of British Insects 10: 1–118.

Barták M, Roháček J (2011) Records of interesting flies (Diptera) attracted to meat baited pyramidal trap on sapping stump of European walnut (*Juglans regia*) in Central Bohemia (Czech Republic). Časopis Slezského Zemského Muzea 60: 223–233. https://doi.org/10.2478/v10210-011-0026-3

Bloxham MG (1978) Notes on Diptera bred from the remains of a nest of *Vespula vulgaris* (common wasp). Bulletin of the Amateur Entomologists' Society 37: 194–196.

Bloxham MG (1982) The Diptera (Calyptratae) of the Sandwell Valley, West Bromwich. In: Chalmers-Hunt JM (Ed.) The Entomologist's Record and Journal of Variation 94: 28–31.

Buenaventura E, Lloyd MW, Perilla López JM, González VL, Thomas-Cabianca A, Dikow T (2021) Protein-encoding ultraconserved elements provide a new phylogenomic perspective of Oestroidea flies (Diptera: Calyptratae). Systematic Entomology 46: 5–27. https://doi.org/10.1111/syen.12443

Calhoun EL, Dodge HR, Fay RW (1956) Description and rearing of various stages of *Dendrophaonia scabra* (Giglio-Tos) (Diptera, Muscidae). Annals of the Entomological Society of America 49: 49–54. https://doi.org/10.1093/aesa/49.1.49

Carvalho de CJB (1989) Classificação de Muscidae (Diptera): uma proposta através da análise cladística. Revista Brasileira de Zoologia 6(4): 627–648. https://doi.org/10.1590/S0101-81751989000400009

Couri MS (2007) A key to the Afrotropical genera of Muscidae (Diptera). Revista Brasileira de Zoologia 24: 175–184. https://doi.org/10.1590/S0101-81752007000100022

Couri MS (2010) Key to the Australasian and Oceanian genera of Muscidae (Diptera). Revista Brasileira de Entomologia 54: 529–544. https://doi.org/10.1590/S0085-56262010000400002

Courtney GW, Sinclair BJ, Meier R (2000) Morphology and terminology of Diptera larvae. In: Papp L, Darvas B (Eds) Contributions to a Manual of Palaearctic Diptera (with Special Reference to Flies of Economic Importance). Science Herald Press, Budapest, Hungary, 85–161.

Cuny R (1978) Muscidae und Calliphoridae (Insecta: Diptera) der Lägern (Schweiz: Jura). Mitteilungen der Schweizerischen Entomologischen Gesellschaft 51: 377–394. https://doi.org/10.5169/seals-401897

Dawson BM, Barton PS, Wallman JF (2020) Contrasting insect activity and decomposition of pigs and humans in an Australian environment: A preliminary study. Forensic Science International 316: 110515. https://doi.org/10.1016/j.forsciint.2020.110515

Emden FI van (1965) The fauna of India and the adjacent countries. Diptera, Muscidae. Government of India, Delhi, 7: 1–647.

Evenhuis NL, Pape T (2023) Systema Dipterorum. In: Bánki O et al. Catalogue of Life Checklist (4.2.2, May 2023). Natural History Museum of Denmark. https://doi.org/10.15468/k7gwad

Fan Z (2008) Fauna Sinica, Insecta vol. 49. Diptera Muscidae (I). Science Press, Beijing, 1–1180.

Ferrar P (1979) The immature stages of dung-breeding muscoid flies in Australia, with notes on the species, and keys to larvae and puparia. Australian Journal of Zoology, Supplementary Series 73: 1–106. https://doi.org/10.1071/AJZS073

Ferrar P (1987) A guide to the breeding habits and immature stages of Diptera Cyclorrhapha. Entomonograph 8: 1–907.

Fuller ME (1932) The larvae of Australian sheep blowflies. Proceedings of The Linnean Society of New South Wales 57: 77–91.

Fuller ME (1934) The insect inhabitants of carrion: a study in animal ecology. Melbourne: Council for Scientific and Industrial Research; Bulletin no. 82: 1–63.

Grzywacz A (2013a) Review and comparative analysis of the morphology of third instar larvae of European and Mediterranean Muscidae (Diptera) of forensic importance. Nicolaus Copernicus University, 1–157.

Grzywacz A (2013b) Third instar larva morphology of *Hydrotaea cyrtoneurina* (Zetterstedt, 1845) (Diptera: Muscidae) – a species of forensic interest. Polish Journal of Entomology 82: 303–315. https://doi.org/10.2478/v10200-012-0044-5

Grzywacz A, Pape T (2013) Morphology of immature stages of *Atherigona reversura* (Diptera: Muscidae), with notes on the recent invasion of North America. Journal of Natural History 47: 1055–1067. https://doi.org/http:10.1080/00222933.2012.742244

Grzywacz A, Pape T (2014) Larval morphology of *Atherigona orientalis* (Schiner) (Diptera: Muscidae) – a species of sanitary and forensic importance. Acta Tropica 137: 174–184. https://doi.org/10.1016/j.actatropica.2014.05.018

Grzywacz A, Lindström A, Hall MJR (2014) *Hydrotaea similis* Meade (Diptera: Muscidae) newly reported from a human cadaver: A case report and larval morphology. Forensic Science International 242: e34–e43. https://doi.org/10.1016/j.forsciint.2014.07.014

Grzywacz A, Wallman JF, Piwczyński M (2017) To be or not to be a valid genus: the systematic position of *Ophyra* R.-D. revised (Diptera: Muscidae). Systematic Entomology 42: 714–723. https://doi.org/10.1111/syen.12240

Grzywacz A, Trzeciak P, Wiegmann BM, Cassel BK, Pape T, Walczak K, Bystrowski C, Nelson L, Piwczyński M (2021) Towards a new classification of Muscidae (Diptera): a comparison of hypotheses based on multiple molecular phylogenetic approaches. Systematic Entomology 46: 508–525. https://doi.org/10.1111/syen.12473

Hardy GH (1939) Notes on Australian Muscoidea (Calyptrata). Proceedings of the Royal Society of Queensland 45: 30–37. https://doi.org/10.5962/p.272112

Haseyama KLF, Wiegmann BM, Almeida EAB, Carvalho de CJB (2015) Say goodbye to tribes in the new house fly classification: A new molecular phylogenetic analysis and an updated biogeographical narrative for the Muscidae (Diptera). Molecular Phylogenetics and Evolution 89: 1–12. https://doi.org/10.1016/j.ympev.2015.04.006

Hennig W (1955) 63 b. Muscidae. In: Lindner E (Ed.) Die Fliegen der Paläarktischen Region. Schweizerbart'sche Verlagsbuchhandlung, Stuttgart, 625–672.

Hennig W (1965) Vorarbeiten zu einem phylogenetischen System der Muscidae (Diptera: Cyclorrhapha). Stuttgarter Beiträge zur Naturkunde 141: 1–100.

Iwasa M, Hori K (1993) A new record of *Potamia littoralis* Robineau-Desvoidy (Diptera: Muscidae) bred from birds' nests in Japan. Japanese Journal of Sanitary Zoology 44(4): 395–396. https://doi.org/10.7601/mez.44.395

Iwasa M, Hori K, Aoki N (1995) Fly fauna of bird nests in Hokkaido, Japan (Diptera). The Canadian Entomologist 127(5): 613–621. https://doi.org/10.4039/Ent127613-5

Jorge SC (2016) Revisão taxonômica e análise cladística do gênero Neotropical *Micropotamia* Carvalho (Diptera, Muscidae). Universidade Federal do Paraná, 1–62.

Keilin D (1917) Recherches sur les Anthomyiidaes a larves carnivores. Parasitology 9(3): 325–450. https://doi.org/10.1017/S0031182000006132

Keilin D, Tate P (1930) On certain semi-carnivorous anthomyid larvae. Parasitology 22(2): 168–181. https://doi.org/10.1017/S0031182000011045

Kovac D, Pont AC, Deeming JC (2023) *Atherigona culicivora*, new species (Insecta: Diptera: Muscidae), a bamboo shoot-fly feeding on mosquito larvae. The Raffles Bulletin of Zoology 71: 583–595. https://doi.org/10.26107/RBZ-2023-0044

Kutty SN, Pape T, Wiegmann BM, Meier R (2010) Molecular phylogeny of the Calyptratae (Diptera: Cyclorrhapha) with an emphasis on the superfamily Oestroidea and the position of Mystacinobiidae and McAlpine's fly. Systematic Entomology 35: 614–635. https://doi.org/10.1111/j.1365-3113.2010.00536.x

Kutty SN, Pont AC, Meier R, Pape T (2014) Complete tribal sampling reveals basal split in Muscidae (Diptera), confirms saprophagy as ancestral feeding mode, and reveals an evolutionary correlation between instar numbers and carnivory. Molecular Phylogenetics and Evolution 78: 349–364. https://doi.org/10.1016/j.ympev.2014.05.027

Kutty SN, Pape T, Pont AC, Wiegmann BM, Meier R (2008) The Muscoidea (Diptera: Calyptratae) are paraphyletic: Evidence from four mitochondrial and four nuclear genes. Molecular Phylogenetics and Evolution 49: 639–652. https://doi.org/10.1016/j.ympev.2008.08.012

Lobanov AM (1965) The morphology of the third instar larvae of the synanthropic flies of the genus *Hydrotaea* R.-D. (Diptera, Muscidae). Zoologicheskii Zhurnal 47: 85–90.

Lobanov AM (1975) On the morphology of the larva *Achanthiptera rohrelliformis* R.-D. (Diptera, Muscidae). Entomologicheskoe Obozrenie 54: 442–445.

Malloch JR (1923) Notes on Australian Diptera with descriptions. [No. i.]. Proceedings of the Linnean Society of New South Wales 48: 601–622.

Malloch JR (1925) Notes on Australian Diptera. [No. vi.]. Proceedings of the Linnean Society of New South Wales 50: 80–97.

McIntosh CS, Dadour IR, Voss SC (2017) A comparison of carcass decomposition and associated insect succession onto burnt and unburnt pig carcasses. International Journal of Legal Medicine 131: 835–845. https://doi.org/10.1007/s00414-016-1464-7

Michelsen V (1977) Oversigt over Danmarks Muscidae (Diptera). Entomologiske Meddelelser 45: 109–163.

Michelsen V (2022) Costal vein chaetotaxy, a neglected character source in Fanniidae and Muscidae (Diptera: Calyptratae). European Journal of Taxonomy 826: 94–134. https://doi.org/10.5852/ejt.2022.826.1839

O'Flynn MA, Moorhouse DE (1980) Identification of early immature stages of some common Queesland carrion flies. Journal of Australian Entomology Society 19: 53–61. https://doi.org/10.1111/j.1440-6055.1980.tb00961.x

Piwczyński M, Pape T, Deja-Sikora E, Sikora M, Akbarzadeh K, Szpila K (2017) Molecular phylogeny of Miltogramminae (Diptera: Sarcophagidae): Implications for classification, systematics and evolution of larval feeding strategies. Molecular Phylogenetics and Evolution 116: 49–60. https://doi.org/10.1016/j.ympev.2017.07.001

Pont AC (1973) Studies on Australian Muscidae (Diptera). IV. A revision of the subfamilies Muscinae and Stomoxyinae. Australian Journal of Zoology, Supplementary Series 21: 129–296. https://doi.org/10.1071/AJZS021

Pont AC (1986) Family Muscidae. In: Soós A, Papp L (Eds) Catalogue of Palaearctic Diptera. Vol. 11. Scatophagidae – Hypodermatidae. Akadémiai Kiadó, Budapest, 57–215.

Pont AC (1989) Family Muscidae. In: Evenhuis NL (Ed.) Catalog of the Diptera of the Australasian and Oceanian Regions. Special Publications of the Bernice Pauahi Bishop Museum 86, Bishop Museum Press, Honolulu. Brill, Leiden, 675–699.

Roback SS (1951) A classification of the muscoid calyptrate Diptera. Annals of the Entomological Society of America 44(3): 327–361. https://doi.org/10.1093/aesa/44.3.327

Roberts MJ (1971) The structure of the mouthparts of some calypterate dipteran larvae in relation to their feeding habits. Acta Zoologica 52: 171–188. https://doi.org/10.1111/j.1463-6395.1971.tb00556.x

Rognes K (1986) A check-list of Norwegian Muscidae (Diptera). Fauna Norvegica Series B 33: 77–85.

Sabrosky CW (1948) The muscid genus *Ophyra* in the Pacific Region (Diptera). Proceedings of the Hawaiian Entomological Society 13: 423–432.

Savage J, Wheeler TA (2004) Phylogeny of the Azeliini (Diptera: Muscidae). Studia Dipterologica 11: 259–299.

Schumann H (1954) Morphologisch-systematische Studien an Larven von hygienisch wichtigen mitteleuropäischen Dipteren der Familien Calliphoridae-Muscidae. Wissenschaftliche Zeitschrift der Universität Greifswald III 1953–54: 245–274.

Séguy E (1923) Diptéres Anthomyides. Faune de France 6: 1–393.

Skidmore P (1973) Notes on the biology of Palaearctic Muscids. The Entomologist 106: 25–59.

Skidmore P (1985) The biology of the Muscidae of the World. Series Entomologica 29: 1–550.

Sorokina VS, Pont AC (2010) An annotated catalogue of the Muscidae (Diptera) of Siberia. Zootaxa 2597: 1–87. https://doi.org/10.11646/zootaxa.2597.1.1

Szpila K, Pape T (2005) The first instar larva of *Apodacra pulchra* (Diptera: Sarcophagidae, Miltogramminae). Insect Systematics & Evolution 36: 293–300. https://doi.org/10.1163/187631205788838447

Szpila K, Walczak K, Johnston NP, Pape T, Wallman JF (2021) First instar larvae of endemic Australian Miltogramminae (Diptera: Sarcophagidae). Scientific Reports 11: 1–12. https://doi.org/10.1038/s41598-020-80139-x

Thomson BCM (1937) Observations on the biology and larvae of the Anthomyiidae. Parasitology 29(3): 273–358. https://doi.org/10.1017/S0031182000024847

Vockeroth JR (1972) A review of the world genera od Mydaeinae, with a revision of the species of New Guinea and Oceania (Diptera: Muscidae). Pacific Insects Monograph 29: 1–134.

Walczak K, Pape T, Ekanem M, Szpila K, Grzywacz A (2023) Insights into the systematics of *Alluaudinella* and allied *Aethiopomyia* and *Ochromusca* (Muscidae, Diptera). Zoologica Scripta 52: 279–297. https://doi.org/10.1111/zsc.12584

Walczak K, Szpila K, Nelson L, Pape T, Hall MJR, Alves F, Grzywacz A (2022) Larval morphology of the avian parasitic genus *Passeromyia*: playing hide and seek with a parastomal bar. Medical and Veterinary Entomology 37: 14–26. https://doi.org/10.1111/mve.12603

Zielke E (2018) On two remarkable species of Azeliinae (Diptera: Muscidae), previously unknown from the Balkans, but collected from Bulgaria already in the 20th century. Historia Naturalis Bulgarica 30: 1–5. https://doi.org/10.48027/hnb.30.01001

Zimin LS (1948) Opredeliteli lichinok sinantropnykh mukh Tadzhikistana. Opredeliteli po Faune CCCP 28: 1–116.

Zumpt F (1965) Myiasis in Man and Animals in the Old World: A Textbook for Physicians, Veterinarians and Zoologists. London: Butterworths, 1–267.